

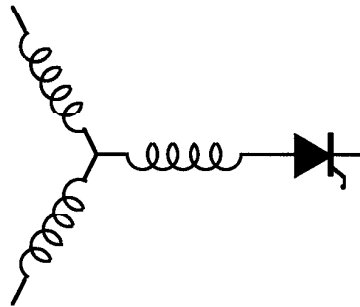
Research Report

**95-17**

**Comparison of Power Production Capability  
Between Doubly Salient Permanent Magnet and  
Variable Reluctance Type Generators**

**B. Sarlioglu and T.A. Lipo**

Wisconsin Power Electronics Center  
University of Wisconsin-Madison  
Madison WI 53706-1691



**W**isconsin  
**E**lectric  
**M**achines &  
**P**ower  
**E**lectronics  
**C**onsortium

University of Wisconsin-Madison  
College of Engineering  
Wisconsin Power Electronics Center  
2559D Engineering Hall  
1415 Johnson Drive  
Madison WI 53706-1691

© March 1995 - Confidential

# Comparison of Power Production Capability Between Doubly Salient Permanent Magnet and Variable Reluctance Type Generators

Bülent ŞARLIOĞLU Thomas A. LIPO

Department of Electrical and Computer Engineering  
University of Wisconsin-Madison  
1415 Johnson Drive  
Madison, WI 53706 USA

**Abstract-** This paper presents a comparison of the power production capability between the newly-conceived Doubly Salient Permanent Magnet (DSPM) generator and a Variable Reluctance machine. The comparison is done by examining the flux-linkage versus current diagrams obtained from a finite element analysis. The machine critical dimensions, i.e., airgap length, inner and outer diameter of stator and rotor etc., the type of steel used in steel laminations, the number of armature winding turns are maintained as identical for a fair comparison. Based on the results of the comparison, it is shown that the doubly salient permanent magnet generator under development promises superior power production capability compared with that of a variable reluctance machine. Consequently, this new type of generator is a promising candidate for power generation where the efficiency, weight and volume of the generator are important concerns.

## I. INTRODUCTION

Doubly salient structures for generation which are normally termed as homopolar inductor alternators have attracted attention in the past for high speed or high frequency applications. These homopolar inductor alternators can be categorized into two groups. In the first group are singly salient machines with conventional sinusoidally distributed stator windings. A typical example for this group is the Lundell generator which is in common use in automobile charging systems. The second category includes doubly-salient alternators which have concentrated, short-pitched stator windings wound around magnetic poles. This type of alternator is sometimes used in high frequency, high speed applications such as aircraft use but is a less developed family of homopolar machines [1,2,3,4].

Since the 1960's, a variety of rare earth magnets have been developed in which the coercive force was dramatically increased by a factor of five while the residual flux density remained almost same as Alnico. However, until recently, these

improved magnets have not been seriously applied to homopolar type structures.

One new motor structure utilizing modern permanent magnets has emerged in the development of novel Doubly Salient Permanent Magnet (DSPM) motor topologies [5,6]. It has been shown that by introducing high flux density permanent magnets in the doubly salient structure of Variable Reluctance Machines (VRM), a new motor geometry can be realized [5]. This topology combines the structural simplicity of a variable reluctance machine and bi-directional conduction operation of the permanent magnet brushless DC motor and appears to afford the possibility of improved performance in terms of torque production and higher efficiency when compared with induction or variable reluctance machines.

The objective of this paper is to convincingly demonstrate the superior power production capability of this novel single phase/two phase doubly salient single phase generator compared to that of a variable reluctance (switched reluctance) type of generator by using the flux linkage versus current diagrams obtained from finite element method analysis. The required power electronics circuitry for converting the ac output terminal quantities into dc quantities is also discussed and compared. The DSPM generator is presently under construction and thus far only design, finite element analysis, and dynamic simulation results have been studied [8].

## II. DSPM GENERATOR CONFIGURATION

Figure 1 illustrates the basic 2-phase, 4/6 pole DSPM generator of the type examined in this paper. It can be noted that the stator of the DSPM generator has four poles. Two permanent magnets are placed inside the stator yoke to provide field excitation for generator action. Permanent magnets are made of high energy density material with a linear demagnetizing characteristic such as that of a rare earth material. For proper operation, permanent magnets must be chosen so that they can, if necessary, sustain the magnetization and demagnetization effects of the armature reaction. The rotor of the basic generator has six poles. Since

there is no winding on the rotor, the structure is clearly very simple and the rotor inertia is small. It can be observed that the six rotor/four stator pole arrangement is effectively the inverse of the four stator/six rotor pole configuration recently reported for motor operation [5,6]. However, the operation of this machine, being essentially a single phase machine, is substantially different than previous DSPM motor topologies.

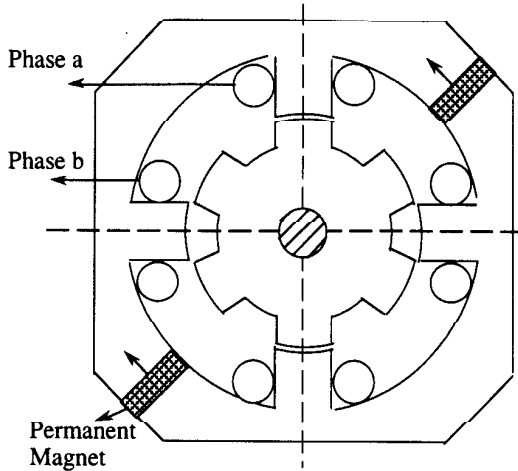


Fig. 1. Magnetic Structure of Doubly Salient Single Phase Permanent Magnet Generator.

It can be noted that since both stator and rotor pole arc are chosen to be same length, ( $\pi/6$  radians), the air gap reluctance seen by the magnet, which contributes the most reluctance, is invariant with rotor position. Therefore, assuming that the PM flux linking each stator winding varies linearly at no load, the voltage induced in the stator windings are trapezoidal (ideally rectangular). When machine is loaded, armature reaction however occurs. This phenomena causes the flux to circulate through the companion overlapped pair as can also be seen in finite element flux contour plots in the forthcoming sections. Consequently, the active stator phase winding has a minimum inductance for a given active stator phase winding occur at both *aligned* and *unaligned* rotor positions. The maximum inductance occurs when the poles are *half overlapped* as shown in Fig. 2.

It will be assumed that, for simplicity, the rate of change of the winding inductance and the PM induced flux of a given active stator phase winding are piece-wise linear and spatially dependent only. This first order approximation is shown in Fig. 2. Because of the overlapped poles, the inductance of each of the windings rises and falls twice during each rise and fall of the magnet flux linking the windings. Note from Fig. 1 that the machine has two independent phases. Fig. 2 shows a plot of the

flux linking the stator phase windings showing the magnet flux linkages with each of the two phases. It can be further noted that the flux linking one of the phase rises (falls) while the flux in the other phase falls (rises). Hence, the emfs induced in the two windings are 180 degree out of phase. Consequently, if these two windings are connected in series such that their emfs polarities add, a simple single phase generator with a square wave emf can be constructed. This type of waveform is clearly ideal when the applications requires such a generator voltage to be rectified since the output voltage of a rectified square wave is a dc voltage with (ideally) no ripple. An illustration of the rectified system configuration is shown in Fig. 3.

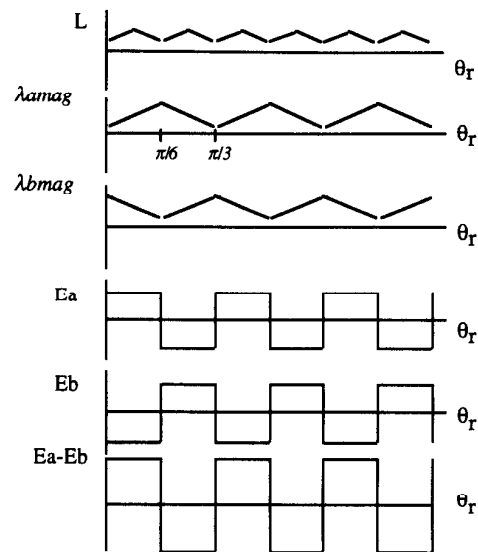


Fig. 2. The phase inductance and permanent magnet flux variations with respect to rotor position of DSPM machine. From top to bottom: L - inductance of phases a and b,  $\lambda_{amag}$ ,  $\lambda_{bmag}$  - magnet flux linking a and b phases,  $E_a$ ,  $E_b$  - emfs induced in a and b windings,  $E_a-E_b$  - series addition of emfs

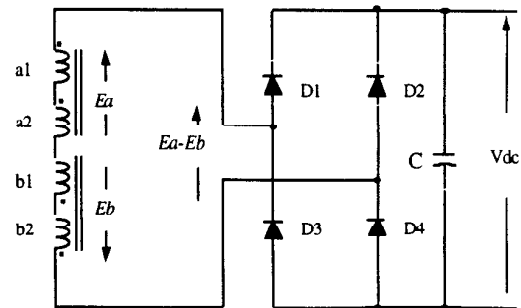


Fig. 3. Generator Phases and Bridge Rectifier Configuration

### III. VR GENERATOR CONFIGURATION

It is clear that a variable reluctance machine can be operated as a motor or a generator depending upon the control strategy. For purposes of illustration, assuming that there is no saturation in the machine, even though that is unlikely and undesirable, the instantaneous torque generation mechanism becomes a function of the square of the phase current and the slope of the phase inductance. Therefore, the only variable that can alter the instantaneous torque polarity is the slope of the phase inductance since the square of current is always positive regardless to the direction of the current itself. Furthermore, if the current is chosen to be unipolar, then the power electronics converter configuration is simplified and the iron loss in the machine can be reduced. Figure 4 illustrates the four stator and six rotor pole VR machine geometry similar to the DSPM machine of Fig. 1.

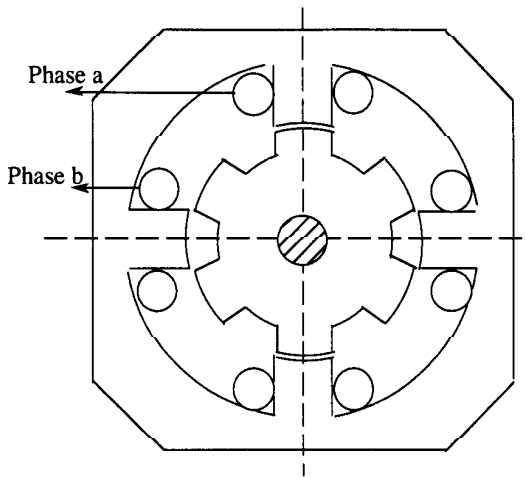


Fig. 4. Magnetic Structure of the Variable Reluctance Generator (VRG).

For generator operation, a current pulse must be sent to each phase when the rotor tooth of that phase leaves the stator tooth, i.e.,  $dL/dt < 0$ . However, since there are no additional windings or permanent magnets establishing a magnetic field the only means available for this purpose is to use again the phase windings itself. During this interval, the total input energy is supplied from both the supply and the shaft, and is stored in the magnetic field. When  $dL/dt < 0$ , all of the stored field energy as well as mechanical energy from the shaft is converted to the electrical energy. It is important to note that during  $dL/dt < 0$ , the mechanical energy is directly converted to the output energy without being stored. The generated power is fed either into an external output terminal or back to the supply depending on the power electronics circuit configuration used. Figure 5 shows the first order approximate waveforms for the phase inductance,

dc link voltage, current waveform, and dc link power.

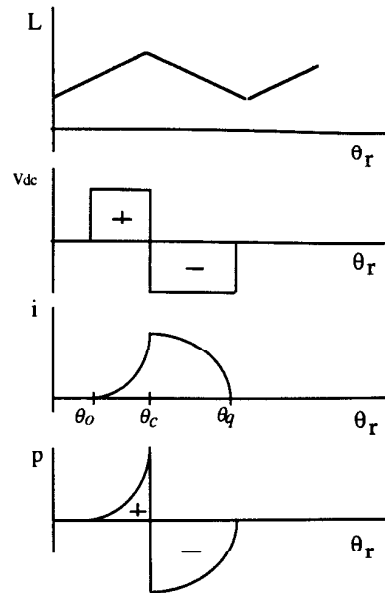


Fig. 5. The phase inductance and power variations with respect to rotor position. From top to bottom:

- L - inductance of a phase
- $V_{dc}$  - dc link voltage
- i - phase current
- p - dc link power

For the generating mode of operation, the electrical output power must surpass the power taken from the supply for magnetizing the iron and for supplying the copper losses. If the losses are ignored this difference comes from the mechanical power supplied by the prime mover. As in the motoring case, at high speeds, the back emf becomes progressively larger, and this reduces the rate of change of the phase current. Therefore turn-on advancing of the phase current pulse is necessary to allow the current to reach its desired value and to try to attain maximum possible output power output. However, too much advance of the current decreases the average output power. In the worst condition, the excitation power requirements becomes equal to the electrical output power, and no net power conversion is achieved. A term 'the excitation penalty' has been defined as being the ratio of the average excitation energy per cycle or "stroke" to the average electrical output energy per stroke and is preferred to be as small as possible [5]. A similar argument is valid for altering the conduction angle  $\theta_c$  of the phase current.

In general, the generated electrical power can either be fed back to the supply, or to an independent output terminal. For the former function, the candidate power electronics converter must both supply and absorb the energy. Some of the converter configurations which carry these

attributes could be an asymmetric bridge, bifilar winding, split source, switched-shared ( $q+1$  switch and 1.5 switch topology) converters. The converters which perform the latter function include the buck or boost configurations in which the non-linear phase inductor (function of current and rotor position) forms the main converter inductor. Each configuration has its own merits and demerits, and must be evaluated based on the specific design requirements. For each function, two examples of the power electronics circuits are shown in Fig. 6.

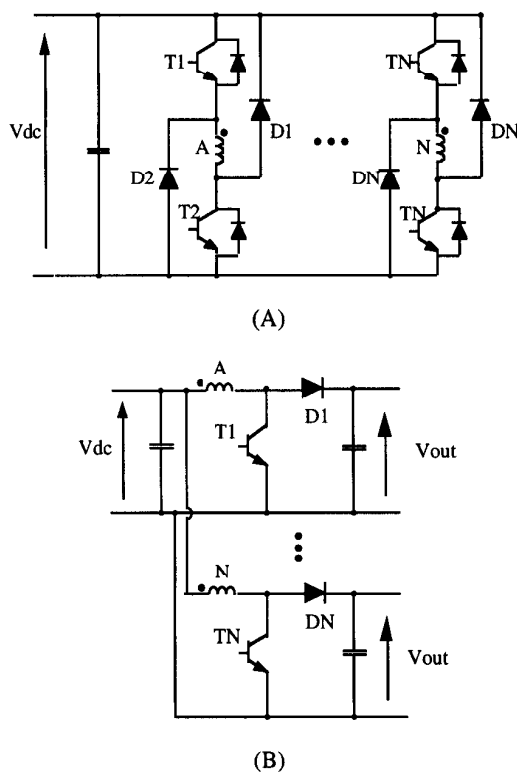


Fig. 6. Power Electronic Circuits for Variable Reluctance Machine  
 A-) Asymmetric Bridge Converter  
 B-) Boost Converter with Auxiliary Excitation ( $V_{dc}$ ) and Machine Phase Winding Used for Commutation Inductance

#### IV. FINITE ELEMENT ANALYSIS

Unfortunately, a performance analysis for the DSPM generator as well as the variable reluctance generator does not fit well into traditionally used methods of analysis such as use of a generalized machine or lumped parameter theories as in the induction, dc or synchronous machines. Both machines are nonlinear due to their geometric doubly salient structure as well as the extensive usage of nonlinear part of the B-H curve, i.e., saturation, of the magnetic materials used.

One means of solving this problem is to use flux-linkage versus current diagrams as has already been successfully utilized to analyze the variable reluctance machines performance. This diagram is obtained by plotting the variation of the instantaneous phase current with respect to the instantaneous phase flux linkage. The data can either be collected by measuring the real quantities via an experiment, or by using a numerical method such as finite element method analysis. The latter approach is advantageous in terms of cost and time since it can be used to verify and improve the electromagnetic design of these machines before construction begins. From either means, the power producing capability of the machine can be calculated and is equal to the area enclosed by the flux linkage vs. current trajectory multiplied by the number of the closed trajectories per revolution of the rotor.

The same electrical and electromagnetic characteristics were chosen to compare the power production capability of the DSPM generator with that of a variable reluctance machine for a fair comparison. The machine dimensions which are kept the same mainly includes, for example, airgap length, inner and outer diameter of stator and rotor copper weight, the type of steel laminations, the number of armature winding turns.

To predict the instantaneous as well as steady state performance, the DSPM and VR type generators have been analyzed by using MSC/EMAS, an electromagnetic finite element analysis package. Zero magnetic vector potentials were imposed on the outer grids of the VRG stator as a boundary condition. However, in order to better include the external leakage effect of the permanent magnet of the DSPM generator, a circular zero magnetic vector potential boundary are used which encircles the stator in the DSPM generator model. The size of the circular boundary condition is maintained as sufficiently large such that neither the required time for the FEM computation and storage will be out of tolerable limits, nor the solution accuracy compromised in the calculation of external leakage of the permanent magnets.

In the two dimensional finite element method analysis, following usual assumptions are made;

- 1) Only the z-component of magnetic vector potential is non-zero while x and y components are zero. Thus the magnetic flux density has two non-zero components. ( $B_x$  and  $B_y$ ),
- 2) The current density is uniform within the armature conductors,
- 3) Because of low operating frequency, displacement currents are negligible,
- 4) The eddy (induced conduction) current in the iron is ignored because of the high resistance of the steel laminations in the axial directions,
- 5) The permeability of the core is isotropic,
- 6) The effect of the bolt holes and other manufacturing defects are ignored.

### A) DSPM & VR Generator Common Dimensions

The geometric quantities used in the FEM analysis are tabulated in TABLE 1. Note that in the FEM analysis, the DSPM mesh model differs from the VRG mesh model with the introduction of a pair of buried permanent magnets in diametrically opposed portions of the stator yoke.

TABLE 1. MAIN DIMENSIONS & OTHER REQUIRED DATA

Stator pole arc	30 degree
Rotor pole arc	30 degree
Airgap length	0.6 mm
Stack length	120 mm
Mean length of stator length	370 mm
Stator outer diameter	200 mm
Stator inner diameter	101 mm
Stator tooth length	34 mm
Rotor tooth length	15 mm
Stator tooth width	26 mm
Rotor tooth width	26 mm
Stacking factor	0.9
Number of turns/phase	24

### B) DSPM & VR Generator Materials

In both FEM models, the rotor and stator laminations are assumed to be made of M36 Electrical Grade steel. For the DSPM generator, the relative permeability of the permanent magnets is assumed to be 1.05 with a coercive force of 800,000 A/m.

### C) DSPM and VR Generator Windings and Excitation.

Each pole is assumed to have one winding with 24 turns of copper wire. Each winding can be considered as having two slots having positive and negative current in the model. For the FEM model of the DSPM generator, the windings are assumed to be connected in series such as one phase is supporting the flux due to the permanent magnet while the other phase is opposing the flux due to the permanent magnet fulfilling Lenz's Law. This sequence depends on the position of rotor with respect to stator (i.e., entering or leaving). For the FEM model of the VR generator, only one phase winding is excited at a time excluding overlap periods.

The FEM analysis was carried out for different rotor angles ranging from full-alignment to full-misalignment for the DSPM generator. The full-alignment of the rotor is assumed to occur at 0 degrees while the full-misalignment occurs at 30 degrees (while the rotor tooth leaves the stator tooth) or -30 degrees (while the rotor tooth comes into alignment with the stator tooth). Note that for the DSPM generator, the FEM solution of one pole flux for the case where the rotor leaves the stator will be the same as for the solution of the adjacent pole for the case the rotor approaches the stator.

For the VR generator, due to the symmetry of the magnetic structure of a phase, it is sufficient to find incremental solutions ranging between full-alignment and full misalignment for cases where only the rotor tooth leaves or approaches the stator tooth.

In the finite element analysis, the quasi-poisson equation for the nonlinear field problem under investigation is solved.

$$\frac{\partial}{\partial x} \left( v \frac{\partial A}{\partial x} \right) + \frac{\partial}{\partial y} \left( v \frac{\partial A}{\partial y} \right) = -J - J_{pm} \quad (1)$$

where  $A$  is the magnetic vector potential in  $z$ -direction,  $v$  is the magnetic reluctivity which is a function of both the magnetic flux density and rotor position, and  $J, J_{pm}$  are the current density vectors in the  $z$  direction due to the armature windings and the permanent magnet respectively. (For a VRM solution,  $J_{pm}$  is zero.) Discretizing the model into first order finite elements and satisfying the functional minimization partial differential equations results in the following matrix equation.

$$[S] \cdot [A] = [T] + [T_{pm}] \quad (2)$$

where  $[S]$  is the stiffness or reluctivity matrix, and  $[A], [T],$  and  $[T_{pm}]$  vectors represents the unknown magnetic vector potentials, nodes associated with triangles enclosing currents, and equivalent nodal current provided by the magnet excitation respectively [7].

For each discrete 3 degree rotor position, five different excitation levels for the armature (or stator for the VRM) winding were formed with the model for the analysis. These armature current levels are in linearly increasing order as follows; no load, i.e., 0 A, and 30 A, 60 A, 90 A, 120 A, and 150 A. Based on the solutions, the flux and its density distribution, and other important physical quantities were obtained for evaluation.

### D) Flux distribution and Magnetic Flux Density

Contour plots of the field variable magnetic vector potential  $A$  are extremely useful in analyzing and visualizing the magnetic field inside a machine. The flux density distribution gives details on the degrees of magnetic saturation, fringing as well as demagnetization. Figure 7 shows the flux plot of the VR generator for the 15 degree rotor position under full-load condition.

Flux plots of the DSPM generator for the same rotor position under no-load and full-load are shown in Fig. 8 and Fig. 9 as an example. For either machine, it can be observed from these plots that, as expected, the flux is mostly concentrated at the stator-rotor teeth overlap region. Another form of illustrating the results would be to look at quantitative values of the flux density distribution inside the machine and in the gap. However, for the convenience of illustrating the results, the flux

plot is chosen here since it does not require a gray or color representation as required to portray the flux density.

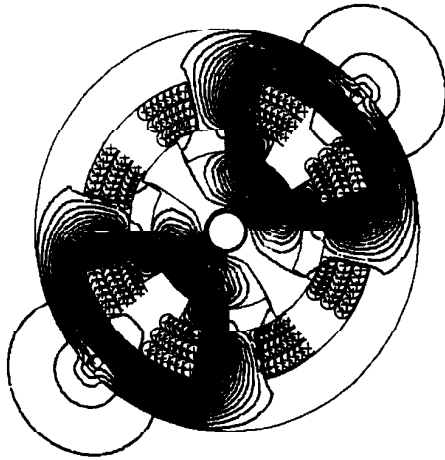


Fig. 7. Flux Plot for Full Load Condition at Half Aligned Rotor Position for VR generator.

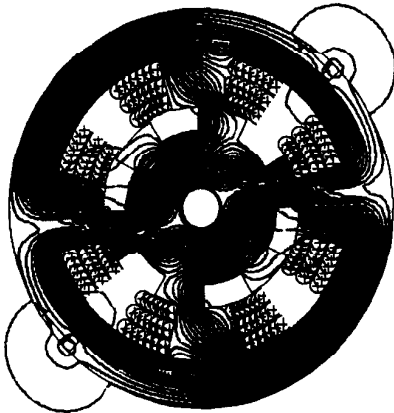


Fig. 8. Flux Plot for No Load Condition at Half Aligned Rotor Position for DSPM generator

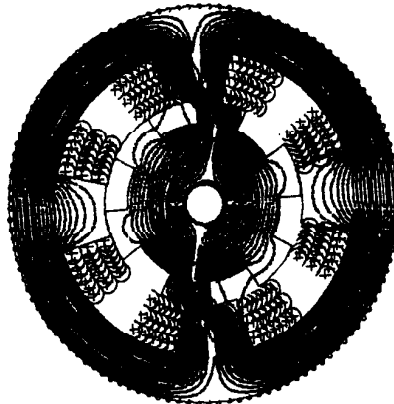


Fig. 9. Flux Plot for Full Load Condition at Half Aligned Rotor Position for DSPM generator.

### E-) Calculation of Flux Linkage

Detailed studies of the magnetic flux linkage of the DSPM generator and VR generator as a function of rotor position and current in the windings have been carried out using the finite element method and the results are shown in Fig. 10 and Fig. 11, respectively.

Figure 10 shows the variation of flux linkage with respect to the armature current for a pole where the rotor teeth is arriving and leaving this particular stator tooth. It can be observed from Fig. 10 plots that the flux on the poles of the DSPM experiences an armature reaction effect. As the stator and rotor poles becomes misaligned, the maximum saturation occurs at the pole tips. Therefore, flux reverses on the adjacent pole. From finite elements, the flux variation within the permanent magnet has been investigated and it has been found that demagnetization is not severe (up to 10% flux change occurs for full load armature current). In Fig. 11, the same variation is shown for the VR generator. Here, it is important to note that the phase flux of the VR generator does return

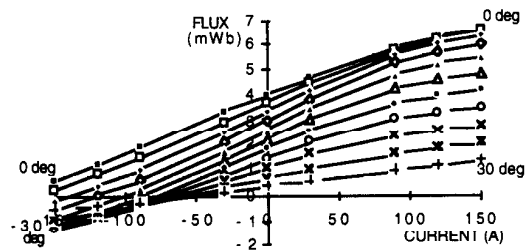


Fig.10 Variation of Flux Linkage of One Armature Phase with Respect to Phase Armature Current and Rotor Position.

0° : Full-alignment of rotor  
30° : Full-misalignment (when rotor leaves stator )  
-30° : Full-misalignment (when rotor comes stator )

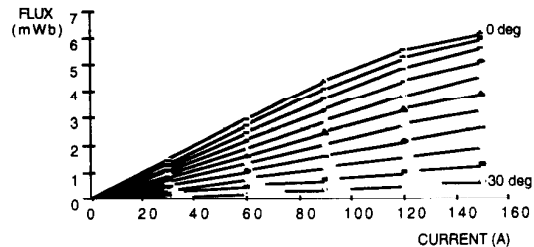


Fig.11 FEM results for VR generator: Variation of Flux Linkage of One Armature Phase with Respect to Phase Armature Current and Rotor Position.

0° : Full-alignment of rotor  
30° : Full-misalignment

to zero when the current becomes zero unlike the phase flux of the DSPM generator. Another observation is that for currents up to some negative level, the phase flux of the DSPM generator still has positive phase flux linkage while the phase flux of the VR machine becomes negative. Further discussion of the flux linkage versus current characteristics in terms of the power production capabilities of these two machines are discussed in the next section.

## V. POWER PRODUCTION CAPABILITIES AND COMPARISON

The instantaneous torque produced by one phase of either machine is equal to the rate of change of the coenergy of that phase with respect to the rotor position when the phase current kept constant, i.e.,

$$T = \left[ \frac{\partial W'}{\partial \theta} \right]_{i=\text{constant}} \quad (3)$$

where  $W'$  is the coenergy and  $\theta$  is the rotor position. From Fig. 12 the coenergy and magnetic field energy respectively are

$$W' = \int_0^i \lambda di \quad (4)$$

$$W = \int_0^\lambda id\lambda \quad (5)$$

The total energy is the sum of the coenergy and magnetic field energy. Power taken or produced is proportional to torque multiplied by the rotor velocity.

$$P = T\omega \quad (6)$$

The generality of these expressions becomes particularly useful when applied to the nonlinear magnetic case. If it is assumed that the current pulse is rectangular, i.e., very fast switching, the coenergy difference between the aligned and unaligned position is the converted energy and is equal to the area traversed by the flux-linkage current trajectory. Therefore, the average electromagnetic torque is equal to the area closed by this trajectory, multiplied by the number of loops per revolution and divided by  $2\pi$ .

$$T = \frac{mN_r}{2\pi} W \quad [\text{Nm}] \quad (7)$$

where  $m$ ,  $N_r$ ,  $W$  are the number of phases, number of the rotor poles, and converted energy (Joules) respectively. If this trajectory is clockwise, this refers to the generator action (negative torque), otherwise, counterclockwise and it refers to motor action (positive torque).

From a design perspective, it can be concluded that the area enclosed by the flux linkage vs. current trajectory, hence the energy conversion,

can be maximized if the aligned flux-linkage is kept as large as possible, and the unaligned flux-linkage as small as possible for the current ranging from no-load to full load.

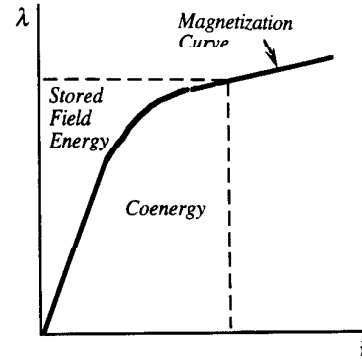


Fig.12 Coenergy, Stored Field Energy and Magnetization Curves

In Fig. 13, the phase flux-linkage vs. current trajectory plots of the DSPM and VR generators are overlaid for purpose of comparison. Here, it has been assumed that the ac output of the DSPM generator supplies a bridge rectifier, i.e., no positive flux exists for negative currents. Consequently, the ratio between the area enclosed by the flux-linkage current locus at full load is

$$\frac{\Delta W'_{\text{DSPM}}}{\Delta W'_{\text{VRG}}} \times 100 \cong 140\% \quad (8)$$

Therefore, for the identical machine geometry and windings, the power production capability of the DSPM generator is 40 % more than that of the VR generator based on this nonlinear comparison. Moreover, another appealing result is that rather than connecting the phase windings in series, if each winding is individually connected to PWM converter, the realization of positive flux at negative currents will be possible and the torque production capability could be increased beyond the value obtained with this comparison.

It is important to note that the term 'capability' is used here since the current in the phase windings can not be changed instantaneously, therefore some of the useful area enclosed will be diminished due to the finite  $di/dt$ . But the effect of finite  $di/dt$  does not change the comparison results dramatically. In reality the DSPM generator has less inductance, hence higher  $di/dt$ , at the aligned position than that of the VR machine. Also, the losses, i.e. copper, iron losses, friction and windage losses in the machines are comparable. However, even in this case the copper losses in the DSPM generator is less as there are not appreciable copper losses associated with magnetization of the stator and rotor iron.



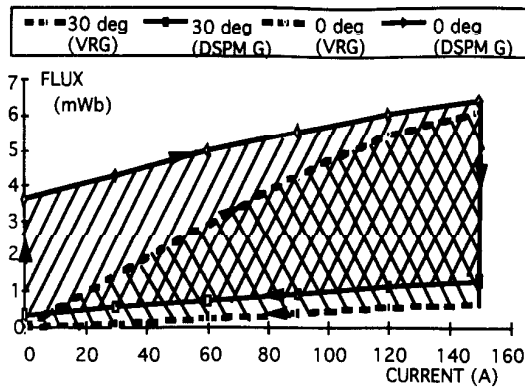


Fig.13 Power Production Comparison of DSPM and VR generators: Variation of Flux Linkage of One Armature Phase with Respect to Phase Armature Current and Rotor Position.

## VI CONCLUSION

In this paper, the power production capability of a newly-conceived DSPM generator is compared with that of a variable reluctance machine by using the flux linkage versus current diagrams obtained from finite element analysis. It has been shown that, by utilizing a high energy density permanent magnet, the doubly salient permanent magnet generator has superior power production capabilities than that of a variable reluctance machine. Consequently, this new type of generator becomes a promising candidate for superior power generation where the efficiency, size, volume and high speed capability of the generator are important. Also the DSPM generator has a very simple magnetic structure which is amenable for low cost manufacturing.

The newly-developed DSPM generator has the advantages over a VR generator as summarized below:

- Higher power output and efficiency than an equivalent VRG.
- No electrical field excitation is necessary, hence no copper losses are associated with field excitation.
- Nearly optimal emf waveform for use in conjunction with a diode bridge rectifier.
- For better performance, a bi-directional mode of operation is possible by using PWM converters (The previous advantage is then not valid for the sake of more power production)

Work is proceeding on the construction of this machine and will be reported in a future paper.

## VII. ACKNOWLEDGMENT

The authors wish to acknowledge gratefully the funding of this project and motivation provided by the Electric Power Research Institute (EPRI) and the Wisconsin Electric Machines and Power Electronics Consortium (WEMPEC) at the University of Wisconsin-Madison.

## REFERENCES

- [1] Walker, J.H., "The Theory of the Inductor Alternator", *Journal of the IEE*, vol. 89, Pt. II, 1942, pp., 227-241.
- [2] Duane, J.T., "A Brushless DC Generator for Aircraft Use", *Trans. AIEE*, Pt II, Nov. 1958, pp. 365-372.
- [3] Rauch, S.E. and Johnson, L.J., "Design Principles of Flux-Switch Alternators", *A.I.E.E. Trans.* Dec. 1955, pp. 1261-1268.
- [4] Zimmerman, R.L., "High Speed Composite Electro-magnet and Permanent Magnet generator", U.S. patent 2,816,240, 1957.
- [5] Liao, Y., Liang, F., and Lipo, T.A., "A Novel Permanent Magnet Motor with Doubly Salient Structure", *IEEE IAS Annual Meeting*, Houston TX, Oct. 5-8, 1992, pp. 308-314.
- [6] Liao, Y., "Design and Performance Evaluation of a New Class of Permanent Magnet machines with Doubly Salient Structure", Ph. D. Thesis, UW Madison, 1992.
- [7] Lipo, T.A., "Electromagnetic Design of AC Machines", Course notes for ECE 713, University of Wisconsin- Madison, 1993
- [8] Sarlioglu, B., Zhao Y., Lipo T.A., "A Novel Doubly Salient Single Phase Permanent Generator", *IEEE IAS Annual Meeting*, Denver, CO, Oct. 2-6, 1994, pp., 9-15.

## APPENDIX

TABLE 2. Data Sheet for the DSPM generator design program

### DSPM GENERATOR ELECTRICAL DATA

Rated current	: 150 A
Rated voltage	: 25 V
Open circuit voltage	: 75 V
Frequency	: 360 Hz.

### CALCULATED MOTOR PARAMETERS AND OTHER IMPORTANT OUTPUTS

Stator wdg. resistance:	0.0068 ohms at 100 degrees Celsius
Minimum inductance	: 0.30 mH
Maximum inductance	: 0.59 mH
Efficiency(%)	: 89.3
Copper losses	: 157.6 W
Iron losses	: 931.7 W
Mechanical losses	: 187.1 W